Kyte, J. (1981) *Nature (London) 292*, 201-204.
Kyte, J., & Doolittle, R. F. (1982) *J. Mol. Biol. 157*, 105-132.
Lowry, O. H., Rosebrough, N. J., Farr, A. L., & Randall, R. J. (1951) *J. Biol. Chem. 193*, 265-275.
Mahoney, W. C., & Hermodson, M. A. (1980) *J. Biol. Chem. 255*, 11199-11203.
Malatesta, F., Darley-Usmar, V., de Jong, C., Prochaska, L. J., Bisson, R., Capaldi, R. A., Steffens, G. C. M., & Buse, G. (1983) *Biochemistry 22*, 4405-4411.
March, S. C., Parikh, I., & Cuatracasas, P. (1974) *Anal. Biochem. 60*, 149-152.
Merrifield, R. B. (1963) *J. Am. Chem. Soc. 85*, 2149-2154.
Merrifield, R. B., Vizioli, L. D., & Boman, H. G. (1982) *Biochemistry 21*, 5020-5031.
Moczydlowski, E. G., & Fortes, P. A. G. (1981) *J. Biol. Chem. 256*, 2346-2356.
Munson, K. B. (1983) *Biochemistry 22*, 2301-2308.
Narita, K., Matsuo, H., & Nakajima, T. (1975) in *Protein Sequence Determination* (Needleman, S. B., Ed.) pp 30-103, Springer-Verlag, New York.
Nicholas, R. N. (1984) *Biochemistry 23*, 888-898.
O'Connell, M. A. (1982) *Biochemistry 21*, 5984-5991.
Ohkawa, I., & Webster, R. E. (1981) *J. Biol. Chem. 256*, 9951-9958.
Penefsky, H. S. (1977) *J. Biol. Chem. 252*, 2891-2899.
Ratnam, M., Nguyen, D. L., Rivier, J., Sargent, P. B., & Lindstrom, J. (1986) *Biochemistry 25*, 2633-2643.
Rifkin, P. B., Compans, R. W., & Reich, E. (1972) *J. Biol. Chem. 247*, 6432-6437.
Rippa, M., Spanio, L., & Pontremoli, S. (1967) *Arch. Biochem. Biophys. 118*, 48-57.
Ross, A. H., Radhakrishnan, R., Robson, R. J., & Khorana, H. G. (1982) *J. Biol. Chem. 257*, 4152-4161.
Sen, A. K., & Post, R. L. (1964) *J. Biol. Chem. 239*, 345-352.
Shapiro, A. L., Viñuela, E., & Maizel, J. V., Jr. (1967) *Biochem. Biophys. Res. Commun. 28*, 815-820.
Sharkey, R. G. (1983) *Biochim. Biophys. Acta 730*, 327-341.
Shull, G. E., Schwartz, A., & Lingrel, J. B. (1985) *Nature (London) 316*, 691-695.
Shull, G. E., Greeb, J., & Lingrel, J. B. (1986) *Biochemistry 25*, 8125-8132.
Stewart, J. M., & Young, J. D. (1969) *Solid Phase Peptide Synthesis*, pp 41-44, W. H. Freeman, San Francisco, CA.
St. John, P. A., Froehner, S. C., Goodenough, D. A., & Cohen, J. B. (1982) *J. Cell Biol. 92*, 333-342.
Wallick, E. T., & Schwartz, A. (1974) *J. Biol. Chem. 249*, 5141-5147.
Walter, G., Scheidtmann, K. H., Carbone, A., Laudano, A. P., & Doolittle, R. F. (1980) *Proc. Natl. Acad. Sci. U.S.A. 77*, 5197-5200.
Weber, K., & Osborn, M. (1969) *J. Biol. Chem. 244*, 4406-4412.
Whittam, R. (1962) *Biochem. J. 84*, 110-118.
Wilchek, M., Bocchini, V., Becker, M., & Givol, D. (1971) *Biochemistry 10*, 2828-2834.
Williams, J. C., Steiner, L. A., Feher, G., & Simon, M. I. (1984) *Proc. Natl. Acad. Sci. U.S.A. 81*, 7303-7307.
Winslow, J. (1981) *J. Biol. Chem. 256*, 9522-9531.

Phosphoenzyme Decomposition in Dog Cardiac Sarcoplasmic Reticulum Ca^{2+}-ATPase†

Taitzer Wang

Department of Pharmacology and Cell Biophysics, University of Cincinnati College of Medicine, Cincinnati, Ohio 45267-0575

Received July 15, 1987; Revised Manuscript Received August 26, 1987

ABSTRACT: A five-syringe quench-flow apparatus was used in the transient-state kinetic study of intermediary phosphoenzyme (EP) decomposition in a Triton X-100 purified dog cardiac sarcoplasmic reticulum (SR) Ca^{2+}-ATPase at 20 °C. Phosphorylation of the enzyme by ATP in the presence of 100 mM K^+ for 116 ms gave 32% ADP-sensitive E_1P, 52% ADP- and K^+-reactive E_2P, and 16% unreactive residual EP_r. The EP underwent a monomeric, sequential $E_1P \xrightarrow{17\ s^{-1}} E_2P \xrightarrow{10.5\ s^{-1}} E_2 + P_i$ transformation and decomposition in the ethylene glycol bis(β-aminoethyl ether)-*N,N,N',N'*-tetraacetic acid quenched Ca^{2+}-devoid medium. The calculated rate constant for the total EP (i.e., $E_1P + E_2P$) dephosphorylation was 7.8 s^{-1}. The E_1P had an affinity for ADP with an apparent $K_d \simeq 100\ \mu M$. When the EP was formed in the absence of K^+ for 116 ms, no appreciable amount of the ADP-sensitive E_1P was detected. The EP comprised about 80% ADP- and K^+-reactive E_2P and 20% residual EP_r, suggesting a rapid $E_1P \rightarrow E_2P$ transformation. Both the E_2P's formed in the presence and absence of K^+ decomposed with a rate constant of about 19.5 s^{-1} in the presence of 80 mM K^+ and 2 mM ADP, showing an ADP enhancement of the E_2P decomposition. The results demonstrate mechanistic differences in monomeric EP transformation and decomposition between the Triton X-100 purified cardiac SR Ca^{2+}-ATPase and deoxycholate-purified skeletal enzyme [Wang, T. (1986) *J. Biol. Chem. 261*, 6307-6319].

In the course of comparative transient-state kinetic studies of SR,[1] we observed that phosphorylation by ATP of the fast-twitch cat caudofemoralis and tibialis and rabbit back muscle SR gave the total acid-stable EP a greater fraction of the ADP-sensitive E_1P than the slow-twitch cat soleus and dog cardiac SR. The rate of the ADP-enhanced decomposition of the ADP-insensitive E_2P in the presence of K^+ was also

† This work was supported by National Institutes of Health Grant P01 HL22619 (IVA-1).

[1] Abbreviations: SR, sarcoplasmic reticulum; EP, phosphoenzyme intermediate of SR Ca^{2+}-ATPase; EGTA, ethylene glycol bis(β-aminoethyl ether)-*N,N,N',N'*-tetraacetic acid.

0006-2960/87/0426-8360$01.50/0

greater in the fast muscle SR than in the slow muscle SR (Wang & Schwartz, 1981; Wang et al., 1981). These data showed that Ca^{2+}-ATPase in the SR microsomes isolated from various muscle types gave EP intermediates of clearly different properties with respect to K^+ and ADP. To pursue these important observations further, we have previously studied in some kinetic detail the EP transformation and decomposition in a deoxycholate-purified skeletal SR Ca^{2+}-ATPase (Wang, 1986a,b), giving a plausible mechanism for explication of the persistent existence of 50% ADP-sensitive E_1P in the total EP and the ADP-enhancement of the total EP decomposition. These observations, which were also made with the detergent-free skeletal microsomes (Wang & Schwartz, 1981; Wang et al., 1981), suggest that there is a tight link between E_1P and E_2P in the form of either a dimeric PE_1E_2P[2] (Wang, 1986a,b) or rapid $E_1P \rightleftarrows E_2P$ with an equilibrium constant $K_e = 1.0$ (see Appendix to this paper).

In this paper, we report the kinetic results obtained with a Triton X-100 purified cardiac SR Ca^{2+}-ATPase, which undergoes EP transformation and decomposition considerably different from those observed with the deoxycholate-purified skeletal enzyme (Wang, 1986a,b). In the proposed sequential $E_1P \rightarrow E_2P \rightarrow E_2 + P_i$ reactions in the cardiac enzyme at 20 °C, the terminating step is considered to be the K^+-catalyzed decomposition of the E_2P (Shigekawa & Dourherty, 1978). The E_1P may interact with ADP yielding E_1 + ATP upon acid quench. This reaction of ADP and E_1P does not appear to affect the E_2P conformer; the E_2P decomposition may be independently enhanced by ADP.

Materials and Methods

[γ-^{32}P]ATP (1 μCi in 0.03 μmol) was purchased from New England Nuclear; ATP and ADP disodium salts were purchased from Boehringer Mannheim. All other chemicals were of chemical pure grade. Glass-distilled deionized water was used.

Preparation of Dog Cardiac SR Ca^{2+}-ATPase. Dog cardiac SR Ca^{2+}-ATPase was purified by solubilization of the crude SR (Sumida et al., 1979; Wang et al., 1979) with Triton X-100 according to the published method (Nakamura et al., 1982; Wang et al., 1984).

General Procedure for Kinetic Experiment. The general procedure for the transient-state kinetic experiments using a five-syringe quench-flow apparatus was described previously in detail (Wang, 1986a). The five syringes were designated SR, ATP, M_1, M_2, and PCA. Briefly, phosphorylation of the SR Ca^{2+}-ATPase by ATP was started in mixer 1 and was allowed to proceed for 116 ms in coil 1. At the end of this reaction, a modifier M_1 (EGTA) was added to chelate the free Ca^{2+} and to quench the EP formation. Following the EGTA quench, the EP decomposition took place for various times in the presence of EGTA in coil 2. The remaining EP was further modified by M_2 (K^+ and/or ADP) and was allowed to decompose for various times in coil 3. The reaction was finally quenched by 9% perchloric acid. Methods for determination of the total acid-stable EP and phosphate ion formed in the reaction were described previously (Sumida et al., 1979; Wang, 1986a). For experiments in which both the EGTA and ADP were placed in the same syringe (syringe M_1), syringe M_2, mixer 3, and coil 3 were omitted. The reaction conditions, the concentrations of the specific reagents in reaction mixtures, and the reaction times in coils 1–3 are stated in the figure legends.

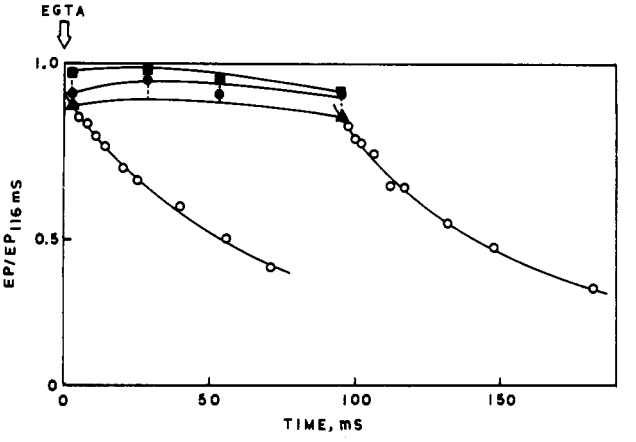

FIGURE 1: Effects of K^+ and ADP on the dog cardiac EP formed in choline chloride. The buffer solution was 20 mM Tris–maleate containing 5 mM NaN_3, pH 6.8. The reaction temperature was 20 °C. The EP was formed for 116 ms in a medium (coil 1) containing 0.05 mg/mL SR Ca^{2+}-ATPase, 10 μM ATP, 100 μM Ca^{2+}, 100 μM EGTA, 3 mM Mg^{2+}, and 30 mM choline cation. The EP_{116ms} was 2.2 nmol/mg. The EP formation was quenched by EGTA and allowed to decompose in a medium (coil 2) containing 3.3 mM EGTA, 3 mM Mg^{2+}, and 30 mM choline cation. At ~2, 18.6, 53.1, and 95.1 ms after EGTA quench, the decomposing EP was incubated with additional choline cation, K^+, or K^+ + ADP for 2.7 ms (coil 3). After each 2.7-ms incubation, the mixture was quenched for determination of EP level: (●) (average of two or three samples) 2.5 mM EGTA, 3 mM Mg^{2+}, and 100 mM choline cation; (■) (average of two or three samples) same as above except 100 mM choline cation was replaced with 77.5 mM K^+ + 22.5 mM choline cation; (▲) (average of two or three samples) same as above with 77.5 mM K^+ and 2 mM ADP. The open circles (○) (4.9, 8.0, 10.5, 14.0, 20.3, 24.9, 39.8, 55.3, and 90 ms after EGTA quench) are the EP decomposition time course in the presence of K^+ + ADP. The solid lines through (○) are computed best fit first-order curves. The solid lines through (●), (■), and (▲) are hand-drawn, and the vertical broken lines indicate the rapid, slight decrease in EP caused by ADP.

Data Analysis. A nonlinear regression computer program, BMD P3R (Jennrich, 1983), was used for analysis of data on EP decomposition, fitting a first-order exponential equation, $EP_t = EP_0e^{-kt} + EP_r$, in which EP_t is the observed total EP at time t, EP_0 is the computed E_2P at $t = 0$ which undergoes first-order decomposition with rate constant k, and EP_r is the residual (time independent) EP. The data in Figures 1 and 2 give best fit numerical values for EP_0, k, and EP_r. The data in Figure 3a give best fit numerical values for EP_0 and k, given a precise value of 0.16 for EP_r. A simulation program for digital computer (TUTSIM, Applied i, Palo Alto, CA) was used for simulation of the time course of $E_1P \rightarrow E_2P \rightarrow E_2 + P_i$ reactions.

Results

The experimental conditions, the concentrations of the reagents, and the amount of the total acid-stable phosphoenzyme formed after 116 ms of phosphorylation of the SR Ca^{2+}-ATPase with ATP (designated EP_{116ms}) are stated in the figure legends.

Effects of K^+ and ADP on EP Formed in the Absence of K^+ (Figure 1). Incubation of the purified dog cardiac SR Ca^{2+}-ATPase with low ATP, low Ca^{2+}, and high Mg^{2+} in a buffer solution containing no added K^+ yielded phosphoenzyme (EP), whose formation could be quenched with EGTA. Incubation of the EP with EGTA for a period of time ranging from ~2 to 95.1 ms did not change the EP level, showing that the EP was stable in a medium containing no K^+ and less than

[2] As noted before [footnote 3 in Wang (1986a)], the subunit E'_1P of the $PE_1E'_1P$ dimer resembles the conventional ADP-insensitive E_2P (Shigekawa & Dourherty, 1978) in many respects. In this paper PE_1E_2P is used in place of $PE_1E'_1P$ for easy comparison with the sequential $E_1P \rightarrow E_2P$ transformation.

Table I: First-Order Kinetics of EP Decomposition under the Influence of ADP (EP Formation Time 116 ms)

figure	ligand condition[a] EP formation	ligand condition[a] EP decomposition	EGTA incubation time (ms)[b]	ADP-sensitive E_1P[c]	k (s^{-1})	E_2P[c,d]	EP_r[c,e]
1	c.c.[f]	K^+; 2 mM ADP	~2	0.01	16.8 ± 2.4	0.82 ± 0.06	0.17 ± 0.07
			95.1	0.04	19.0 ± 2.3	0.76 ± 0.04	0.20 ± 0.05
2	K^+	K^+; 2 mM ADP	~2	0.31	22.6 ± 9.3	0.47 ± 0.08	0.22 ± 0.09
			18.6	0.24	16.8 ± 4.8	0.52 ± 0.07	0.14 ± 0.08
			53.1	0.13	[g]	[g]	[g]
			95.1	0.06	20.8 ± 5.4	0.37 ± 0.04	0.13 ± 0.04
3a	K^+	K^+; 0 μM ADP	0[h]	0	7.5 ± 0.8	0.86 ± 0.02	0.16[i]
		K^+; 30 μM ADP	0	0.04	12.2 ± 1.1	0.80 ± 0.03	0.16
		K^+; 120 μM ADP	0	0.16	15.2 ± 1.2	0.68 ± 0.02	0.16
		K^+; 1000 μM ADP	0	0.28	19.1 ± 1.4	0.56 ± 0.02	0.16

[a] See figure legends for other ligands. [b] Incubation time after EGTA quenching of EP. [c] Based on EP_{116ms} = 1.0. [d] The fraction of EP associated with k. [e] Computed residual (time independent) fraction of EP. [f] c.c., choline chloride. [g] Not computed, due to scattering of data. [h] EGTA was added together with ADP. [i] Average of the three mean values of EP_r derived from the data in Figure 2.

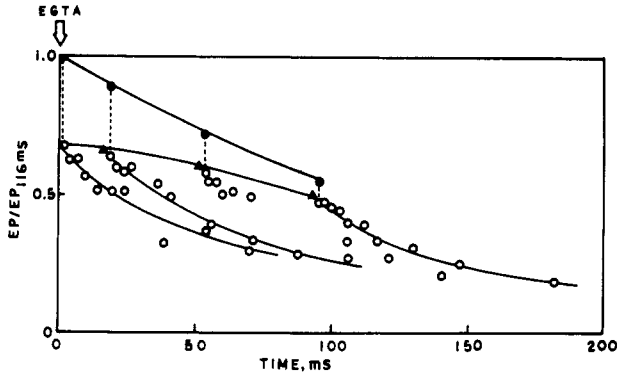

FIGURE 2: Effect of ADP on the dog cardiac EP formed in K^+. The buffer solution was 20 mM Tris–maleate containing 5 mM NaN_3, pH 6.8. The reaction temperature was 20 °C. The EP was formed for 116 ms in a medium (coil 1) containing 0.08 mg/mL SR Ca^{2+}-ATPase, 10 μM ATP, 100 μM Ca^{2+}, 100 μM EGTA, 3 mM Mg^{2+}, and 100 mM K^+. The EP_{116ms} was 2.2 nmol/mg. The EP formation was quenched with EGTA and allowed to decompose in a medium (coil 2) containing 3.3 mM EGTA, 3 mM Mg^{2+}, and 100 mM K^+. At ~2, 18.6, 53.1, and 95.1 ms after EGTA quench, the decomposing EP was incubated with K^+ or K^+ + ADP for 2.7 ms (coil 3). After each 2.7-ms incubation, the mixture was quenched for determination of EP level: (●) (average of two or three samples) 2.5 mM EGTA, 3 mM Mg^{2+}, and 100 mM K^+; (○) (average of two or three samples) same as above with 2 mM ADP followed by 4.9, 8.0, 10.5, 14.0, 20.3, 24.9, 39.8, 55.3, and 90.0 ms. The solid lines through (○) are computed best fit first-order decomposition curves, each of which gives an extrapolated EP (▲) at t = 0 ms. The vertical broken lines indicate the rapid decrease in EP by ADP, representing the amounts of E_1P at various points after EGTA quenching. The solid lines through (●) and (▲) are simulated time courses of $E_1P + E_2P + EP_r$ and $E_2P + EP_r$, respectively, on the basis of sequential $E_1P \xrightarrow{k_1} E_2P \xrightarrow{k_2} E_2 + P_i$ reactions with EP_r (which is not included in the transformation) assumed to be constant at 0.16. At time zero, E_1P = 0.32 and E_2P = 0.52. The rate constants that generate the curves are k_1 = 17 s^{-1} and k_2 = 10.5 s^{-1}.

1 mM free Mg^{2+}. Addition of K^+ at various points of EGTA incubation caused no rapid decrease in EP. On the other hand, addition of K^+ + ADP caused a rapid decrease in EP of no more than 5% of EP_{116ms}, showing that only a small amount of ADP-sensitive E_1P was present. Under these conditions, regardless of how long the original EP had been incubated with EGTA, nearly 80% of the E_2P decomposed with similar rate constants. The remaining 17–20% EP appeared to be stable in the presence of ADP and K^+. The computed first-order rate constants and various EP fractions are listed in Table I.

In separate experiments carried out in the buffer solutions containing Li^+ [which replaced choline cation so that the P_i formed in the medium could easily be extracted with acidic ammonium molybdate and butanol (Wang, 1986a)], the E_2P reacted with ADP + K^+ and released P_i in nearly the stoichiometric amount (data not shown).

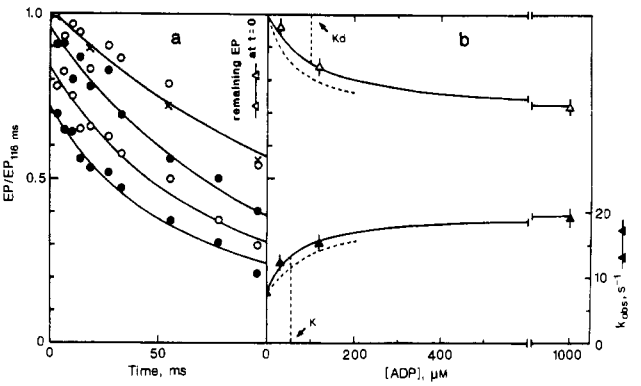

FIGURE 3: (a) Decomposition of dog cardiac EP at various ADP concentrations. Experimental conditions are the same as in Figure 2 except that the formation of EP was quenched with EGTA + ADP and allowed to decompose in coil 2 before final quenching with perchloric acid. The following ADP concentrations were used [(○) and (●) from top to bottom]: 0, 30, 120, and 1000 μM. The solid lines through the circles are computed first-order EP decompositions: $EP_t = EP_0e^{-kt} + 0.16$. The four data points symbolized (×) are taken from Figure 2 (●); they are included for comparison. (b) (△) Plot of [ADP·E_1P] versus [ADP] ([ADP·E_1P] = $[EP]_{total}$ − [EP] remaining at t = 0). The solid curve is computed on the basis of the hyperbolic equation $[ADP\cdot E_1P] = [E_1P]_{max}[ADP]/(K_d + [ADP])$ with $[E_1P]_{max}$ = 0.3 and K_d = 100 μM. The broken curve was based on the same E_1P_{max} and K_d = 55 μM. (▲) Plot of k_{obsd} versus [ADP]. The solid curve is computed on the basis of the hyperbolic equation $k_{obsd} = k_0 + (k_{obsd,max} - k_0)[ADP]/(K + [ADP])$ with k_0 = 7.5 s^{-1}, $k_{obsd,max}$ = 19.5 s^{-1}, and K = 55 μM. The broken curve is based on the same k_0 and $k_{obsd,max}$ and K = 100 μM.

Effects of K^+ and ADP on EP Formed in the Presence of K^+ (Figures 2 and 3). The kinetic properties of the EP formed in the presence of high K^+ (Figure 2) were clearly different from those of the EP formed in the absence of K^+. The EP, when incubated in EGTA + K^+ medium for 95.1 ms, decreased by 40%. Addition of 2 mM ADP at various points of EGTA + K^+ incubation revealed the existence of the ADP-sensitive E_1P, which was 32% of EP_{116ms} at the time of EGTA quenching but decreased to 5% at 95.1 ms after EGTA quenching. In each case, the remaining EP comprised two EP fractions, one of which decomposed with a rate constant similar to that of the E_2P formed in the absence of K^+ (Figure 1). The other fraction appeared to be stable, accounting for 13–22% of the total EP. The computed first-order rate constants and various fractions of EP are listed in Table I.

On the basis of the sequential $E_1P \xrightarrow{k_1} E_2P \xrightarrow{k_2} E_2 + P_i$ mechanism and simulation of EP time course with zero time values of $[E_1P]$ = 0.32, $[E_2P]$ = 0.52, and $[EP_r]$ = 0.16 (which is the average of the three mean values of EP_r given in Table

I), the rate constant k_1 for the $E_1P \rightarrow E_2P$ transformation was estimated to be 17 s^{-1}, the rate constant k_2 for the E_2P decomposition was 10.5 s^{-1}, and the apparent rate constant k_{app} for the decomposition of the total EP (i.e., $E_1P + E_2P$) was 7.8 s^{-1}.

When EGTA and various amounts of ADP were added simultaneously to the EP that had been formed for 116 ms, various amounts of the initial burst of EP disappearance and various observed rate constants of the slow-phase EP decomposition were observed (Figure 3a). The computed first-order rate constants and various fractions of EP are listed in Table I. The rate constant (7.5 ± 0.8 s^{-1}) at [ADP] = 0 μM is consistent with the simulated $E_1P + E_2P$ decomposition rate constant given above, so are the E_1P fraction (0.28) and the rate constant (19.1 ± 1.4 s^{-1}) for the slow-phase EP decomposition at [ADP] = 1 mM. As shown in Figure 3b, using 0.3 as the maximum fraction of E_1P, the plot of [ADP·E_1P] (i.e., $[EP]_{total}$ − [EP] remaining at $t = 0$) versus [ADP] fits $[ADP \cdot E_1P] = 0.3[ADP]/(K_d + [ADP])$ with K_d = 100 μM. The plot of k_{obsd} versus [ADP] may fit $k_{obsd} = 7.5\ s^{-1} + (12\ s^{-1})[ADP]/(K + [ADP])$ with K = 55 μM, when the rate constant of 19.5 s^{-1} (an average value obtained at [ADP] = 2 mM; cf. Figure 2 and Table I) is used as a maximum. The K_d and K are significantly different, as can be seen by comparing the solid and the broken hyperbolic curves in the figure.

Discussion

The new data on EP decomposition suggest that the Triton X-100 purified dog cardiac SR EP may undergo sequential $E_1P \rightarrow E_2P \rightarrow E_2 + P_i$ reactions at 20 °C, similar to the skeletal EP sequential decomposition at 0 °C proposed by Shigekawa and Dourherty (1978). As in the skeletal SR at 0 °C (Shigekawa & Dourherty, 1978), the cardiac $E_1P \rightarrow E_2P$ transformation in the absence of K^+ is also rapid and appears to be irreversible. However, the EP decomposition in the cardiac SR Ca^{2+}-ATPase is considerably different from that in the deoxycholate-purified skeletal enzyme at 20 °C (Wang, 1986a), studied by the same five-syringe quench-flow methodology. The following discussion considers two plausible reaction mechanisms, which reveal important intrinsic properties of the intermediary EP in the two purified enzyme preparations.

In the sequential mechanism (eq 1) derived from the cardiac

$$E_1P \xrightarrow{17\ s^{-1}} E_2P \xrightarrow{10.5\ s^{-1}} E_2 + P_i \quad (1)$$

$$E_1P \underset{}{\overset{K_e = 1.0}{\rightleftharpoons}} E_2P \xrightarrow{28.8\ s^{-1}} E_2 + P_i \quad (2)$$

data, the first-formed ADP-sensitive E_1P may transform to the ADP- and K^+-reactive E_2P[3,4] with a rate constant of 17 s^{-1}, predominantly in the forward direction. The E_2P may in turn decompose at 10.5 s^{-1} in the terminating step, nearly 2 times slower than the preceding $E_1P \rightarrow E_2P$ transition. It is demonstrable by skeletal data (Wang, 1986a) that at 20 °C the transformation of E_1P and E_2P may be readily reversible and that both the forward and reverse rates are much greater than the terminating E_2P decomposition (eq 2) [see the Appendix for the derivation of this monomeric reaction mechanism from the data which also support a dimeric interactive dephosphorylation in the skeletal enzyme previously reported by Wang (1986a,b)]. The decomposition rate of the monomeric skeletal E_2P is nearly 3 times that of the cardiac E_2P. Both mechanisms postulate that the E_1P does not decompose without transforming to E_2P (Shigekawa & Dourherty, 1978; Hobbs et al., 1985).

In view of the documented evidence that the E_1P and E_2P may contain occluded Ca^{2+} (Takakuwa & Kanazawa, 1982; Takisawa & Makinose, 1983; Dupont, 1980; Nakamura, 1987), it is reasonable to suggest that the rate of Ca^{2+} translocation in the sequential mechanism (eq 1) is determined by the overall $E_1P + E_2P$ decomposition, whose apparent first-order rate constant is computed to be 7.8 s^{-1}. This value is smaller than that of the overall $E_1P + E_2P$ decomposition, 14.4 s^{-1}, observed with the skeletal enzyme (eq 2). Judging from the speculated rate constants for Ca^{2+} translocation [7.8 s^{-1} for the cardiac SR and 14.4 s^{-1} for the skeletal SR (Wang, 1986a; Froehlich & Heller, 1985; Chiu & Haynes, 1980)], one can rationalize that the Ca^{2+} translocation across the SR membrane may occur at a lower rate in the cardiac than in the skeletal SR Ca^{2+} pump, disregarding any effect of the detergent used in each enzyme preparation.

By using ADP as a probe, we observed that the cardiac E_1P had an affinity for ADP with $K_d \simeq 100\ \mu$M, similar to that of the deoxycholate-purified skeletal E_1P (Wang, 1986a). This suggests that the ADP-sensitive E_1P conformer of the cardiac and skeletal Ca^{2+}-ATPases has a similar binding site for ADP. Both presumptive ADP·E_1P complexes are acid-labile. In spite of these similarities, the subsequent $E_1P \rightarrow E_2P$ transformation may be different as shown in eq 1 and 2. Judging from the fact that the cardiac E_2P decomposes at similar rate in the presence of ADP, K^+, and a wide range of E_1P (1–31%), we tentatively conclude that ADP may not enhance the E_1P decomposition. It appears likely that the apparent ADP-enhanced EP decomposition is largely due to the interaction of ADP and E_2P, giving P_i as the major product (Shigekawa & Dourherty, 1978; Hobbs et al., 1985), and that ADP may stabilize the E_1P conformer (ADP·E_1P dephosphorylates presumably only upon acid quench) as shown in eq 3. In

$$ATP + E_1 \not\leftrightarrow ADP \cdot E_1P \not\leftrightarrow ADP \cdot E_2P \xrightarrow{19.5\ s^{-1}} E_2 + P_i + ADP \quad (3)$$

$$ATP + E_1 \xleftarrow{58.2\ s^{-1}} ADP \cdot E_1P \overset{K_e = 1.0}{\rightleftharpoons} ADP \cdot E_2P \xrightarrow{28.8\ s^{-1}} E_2 + P_i + ADP \quad (4)$$

contrast, the skeletal data suggest that both ADP·E_1P and ADP·E_2P complexes may exist in a rapid equilibrium. ADP enhances the E_1P decomposition but does little to the E_2P as shown in eq 4. The latter type of ADP-enhanced E_2P decomposition by way of its transformation to ADP·E_1P does not seem to be viable in the cardiac Ca^{2+}-ATPase, as evidenced by the fact that the two hyperbolic plots of [ADP·E_1P] and k_{obsd} versus [ADP] give two different ADP concentrations at half-maximum [ADP·E_1P] and k_{obsd}. The cardiac data give $K_d \neq K$ (Figure 3b), disallowing estimation of the affinity of E_2P for ADP by the same analysis used in the skeletal enzyme (Wang, 1986a,b).

Although the kinetic results of EP transformation and decomposition show that the Triton X-100 purified cardiac SR Ca^{2+}-ATPase is different from the deoxycholate-purified

[3] The conventional ADP-insensitive E_2P (Shigekawa & Dourherty, 1978) is referred to as ADP- and K^+-reactive E_2P in this paper to indicate that this fraction of the total EP is reactive to both ADP and K^+, an experimental observation that was also recently reported by Hobbs et al. (1985).

[4] The well-documented E–P → E·P → E + P_i conversion is not included in the reaction mechanism for the following reasons: (1) The kinetic mechanism is derived from E–P decomposition, which gives the only experimentally (by acid quench) observable time course. (2) Upon acid quench the intermediate E·P is observed as the end products E + P_i; therefore, to distinguish the two steps in the conversion on the basis of E–P decomposition would be an overinterpretation of the data in these kinetic studies.

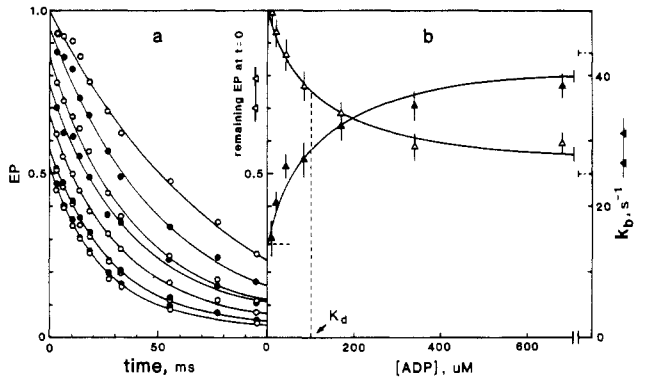

FIGURE 4: (a) Decomposition of rabbit skeletal EP at various ADP concentrations (0–680 μM). (b) Symbols (△) and (▲) are the same as described in Figure 3. Nonlinear regression data analysis on the basis of the hyperbolic equations yields $[E_1P]_{max} = 0.5 \pm 0.01$, $k_0 = 14.4 \pm 2.2$ s^{-1}, $k_{obsd\,max} = 43.5 \pm 4.4$ s^{-1}, and $K_d = 100 \pm 11$ μM (△) and 101.6 ± 32 μM (▲) (Wang, 1986a).

skeletal enzyme (Wang, 1986a,b), it is not clear whether or not these differences reflect the monomeric and oligomeric states (Briggs, 1986; Ikemoto, 1982) of the two enzyme proteins. Nor are the detergent effects (McIntosh & Davidson, 1984; Champeil et al., 1986) known on these two solubilized enzymes. So far as the enzyme proteins are concerned, the observed kinetic differences appear to be in accordance with the recent findings that amino acid sequences of the cardiac and the fast-twitch skeletal SR Ca^{2+}-ATPases are different (Brandl et al., 1986; MacLennan et al., 1985; DeFoor et al., 1980), mostly in the N-terminus, ATP binding, and phosphorylation domains (Brandl et al., 1986). However, since the lipid components of the SR membranes play important roles in ATP hydrolytic activities of the Ca^{2+}-ATPase (Moore et al., 1981; Bennett et al., 1978; Meissner & Fleischer, 1972; Messineo et al., 1984; Hidalgo et al., 1986), the differences in EP decomposition between the two enzymes described in this work may in part be due to different effects of lipid components on E_1P and E_2P. Our preliminary results are consistent with this premise. Inclusion of skeletal SR lipids in the resealed cardiac SR (from the Triton X-100 solubilized enzyme) results in a twofold increase in the E_1P fraction, but the E_2P decomposition is not enhanced to the same extent[5] as would be expected in the skeletal enzyme.

ACKNOWLEDGMENTS

I express my special gratitude to Dr. Arnold Schwartz for his continuing encouragement and support of my transient-state kinetic studies on SR and to Liz Wendelmoot for her help in preparing the manuscript.

APPENDIX

We have previously reported a dimeric reaction mechanism for the deoxycholate-purified SR Ca^{2+}-ATPase on the basis of the data summarized in Figure 4 (Wang, 1986a). The explicit kinetic scheme is shown in eq 5.

$$\begin{array}{ccccccc} PE_1E_2P + ADP & \overset{K_d = 100\,\mu M}{\rightleftharpoons} & ADP{\cdot}PE_1E_2P & \xrightarrow{29.1\ s^{-1}} & E_1E_2 + ATP + P_i \\ \downarrow 14.4\ s^{-1} & & \downarrow 14.4\ s^{-1} & & \\ E_1E_2 + 2P_i & & E_1E_2 + ATP + P_i & & \end{array} \quad (5)$$

Favoring the monomeric Ca^{2+}-ATPase as a functional unit for the skeletal enzyme, one can resolve the dimeric PE_1E_2P into two monomers which exist in equal amount in a rapid equilibrium, $E_1P \rightleftarrows E_2P$, persisting throughout the dephosphorylation. Unlike the dimeric PE_1E_2P which produces 2 mol of P_i with a rate constant of 14.4 s^{-1}, the reactive, monomeric E_2P gives only 1 mol of P_i in the rate-determining step. Therefore, to account for the rate of total EP disappearance, the E_2P decomposition rate constant should be twice as great as that of the PE_1E_2P disappearance. Equation 5′ (i.e., eq 5 at [ADP] = 0) then becomes eq 2.

$$PE_1E_2P \xrightarrow{14.4\ s^{-1}} E_1E_2 + 2P_i \quad (5')$$

The alternative monomeric mechanism (eq 2) must also match the theoretical requirements and experimental data from which the dimeric mechanism (eq 5) (Wang, 1986a,b) of the reaction of ADP and PE_1E_2P is derived. For this reason, it is necessary to consider that both E_1P and E_2P bind ADP and that the resultant ADP·E_1P and ADP·E_2P also exist in a rapid equilibrium and undergo the dephosphorylation as shown in eq 4.

To fit the data, one should also consider that E_1P and E_2P have the same affinity for ADP ($K_d = 100$ μM ADP). Thus, combining the two equilibria given in eq 2 and 4, the complete reaction scheme for the reactions of monomeric E_1P and E_2P with ADP can be written as

$$\begin{array}{ccccc} E_1P & \overset{K_e = 1.0}{\rightleftharpoons} & E_2P & \xrightarrow{28.8\ s^{-1}} & E_2 + P_i \\ K_d = 100\,\mu M \downarrow\uparrow & & \downarrow\uparrow K_d & & \\ ADP{\cdot}E_1P & \overset{K_e}{\rightleftharpoons} & ADP{\cdot}E_2P & \xrightarrow{28.81\ s^{-1}} & E_2 + P_i + ADP \\ \downarrow 58.2\ s^{-1} & & & & \\ E_1 + ATP & & & & \end{array}$$

Kinetically, this complete equilibrium scheme is indistinguishable from the dimeric interactive dephosphorylation shown in eq 5, because both mechanisms are supported by the same set of data (Wang, 1986a) in Figure 4. These data yield equal K_d values from plots of [ADP·E_1P] and k_{obsd} versus [ADP], allowing estimation of the affinity of the skeletal E_2P for ADP.

The above-detailed analyses based on the principle of chemical kinetics allow one to gain insight into plausible SR Ca^{2+}-ATPase reaction mechanisms, which may reveal important properties of the intermediary phosphoenzymes.

[5] T. Wang, unpublished experiments.

REFERENCES

Bennett, J. P., Smith, G. A., Houslay, M. D., Hesketh, J. C., Metcalfe, J. C., & Warren, G. B. (1978) *Biochim. Biophys. Acta 513*, 310–320.

Brandl, C. J., Green, N. M., Korczak, B., & MacLennan, D. H. (1986) *Cell (Cambridge, Mass.) 44*, 597–607.

Briggs, F. N. (1986) *Cell Calcium 7*, 249–260.

Champeil, P., le Maire, M., Andersen, J. P., Guillain, F., Gingold, M., Lund, S., & Moller, J. V. (1986) *J. Biol. Chem. 261*, 16372–16384.

Chiu, V. C. K., & Haynes, D. H. (1980) *J. Membr. Biol. 56*, 219–239.

DeFoor, P. H., Levitsky, D., Biryukova, T., & Fleischer, S. (1980) *Arch. Biochem. Biophys. 200*, 196–205.

Dupont, Y. (1980) *Eur. J. Biochem. 109*, 231–238.

Froehlich, J. P., & Heller, P. F. (1985) *Biochemistry 24*, 126–136.

Hidalgo, C., De La Fuente, M., & Gonzalez, M. E. (1986) *Arch. Biochem. Biophys. 247*, 365–371.

Hobbs, A. S., Albers, R. W., Froehlich, J. P., & Heller, P. F. (1985) *J. Biol. Chem. 260*, 2035–2037.

Ikemoto, N. (1982) *Annu. Rev. Physiol. 44*, 297–317.

Jennrich, R. (1983) in *BMD P3R Nonlinear Regression, BMDP Statistical Software* (Dixon, W. J., Ed.) pp 290–304, University of California Press, Berkeley, Los Angeles, and London.
MacLennan, D. H., Brandl, C. J., Korczak, B., & Green, N. M. (1985) *Nature (London) 316*, 696–700.
McIntosh, D. B., & Davidson, G. A. (1984) *Biochemistry 23*, 1959–1965.
Meissner, G., & Fleischer, S. (1972) *Biochim. Biophys. Acta 255*, 19–33.
Messineo, F. C., Rathier, M., Favreau, C., Watras, J., & Takenaka, H. (1984) *J. Biol. Chem. 259*, 1336–1343.
Moore, B. M., Lentz, B. R., Hoechli, M., & Meissner, G. (1981) *Biochemistry 20*, 6810–6817.
Nakamura, J. (1987) *J. Biol. Chem. 262*, 14492–14497.
Nakamura, J., Wang, T., Tsai, L. I., & Schwartz, A. (1983) *J. Biol. Chem. 258*, 5079–5083.
Shigekawa, M., & Dourherty, J. P. (1978) *J. Biol. Chem. 253*, 1458–1464.
Sumida, M., Wang, T., Mandel, F., Froehlich, P. J., & Schwartz, A. (1979) *J. Biol. Chem. 253*, 8772–8777.
Takakuwa, Y., & Kanazawa, T. (1982) *J. Biol. Chem. 256*, 426–431.
Takisawa, H., & Makinose, M. (1983) *J. Biol. Chem. 258*, 2986–2992.
Wang, T. (1986a) *J. Biol. Chem. 261*, 6307–6316.
Wang, T. (1986b) *J. Biol. Chem. 261*, 6317–6319.
Wang, T., & Schwartz, A. (1981) *Biochim. Biophys. Acta 638*, 341–344.
Wang, T., Tsai, L. I., Solaro, R. J., Grassi de Gende, A. O., & Schwartz, A. (1979) *Biochem. Biophys. Res. Commun. 91*, 356–361.
Wang, T., Grassi de Gende, A. O., Tsai, L. I., & Schwartz, A. (1981) *Biochim. Biophys. Acta 637*, 523–529.
Wang, T., Nakamura, J., & Schwartz, A. (1984) in *Methods in Pharmacology* (Schwartz, A., Ed.) Vol. 5, Chapter 4, pp 39–47, Plenum, New York.

Analysis of Positional Isotope Exchange in ATP by Cleavage of the βP–OγP Bond. Demonstration of Negligible Positional Isotope Exchange by Myosin†

Marsha P. Dale‡ and David D. Hackney*
Department of Biological Sciences, Carnegie Mellon University, Pittsburgh, Pennsylvania 15213
Received April 20, 1987; Revised Manuscript Received July 28, 1987

ABSTRACT: A method for analysis of positional isotope exchange (PIX) during ATP ⇌ HOH oxygen exchange is presented that uses a two-step degradation of ATP resulting in cleavage of the βP–OγP bond. This cleavage yields P_i derived from the γ-phosphoryl of ATP that contains all four of the γ oxygens. Both PIX between the β,γ-bridge and β-nonbridge positions and washout of the γ-nonbridge oxygens can be simultaneously followed by using ATP labeled with ^{17}O at the β-nonbridge positions and ^{18}O at the β,γ-bridge and γ-nonbridge positions. Application of this method to ATP ⇌ HOH exchange during single turnovers of myosin indicates that the bulk of the ATP undergoes rapid washout of γ-nonbridge oxygens in the virtual absence of PIX. At 25 °C with subfragment 1 the scrambling rate is at the limit of detectability of approximately 0.001 s^{-1}, which is 50-fold slower than the steady-state rate. This corresponds to a probability of scrambling for the β-oxygens of bound ADP of 1 in 10000 for each cycle of reversible hydrolysis of bound ATP. A fraction of the ATP, however, does not undergo rapid washout. With myosin and stoichiometric ATP at 0 °C, this fraction corresponds to 10% of the ATP remaining at 36 s, or 2% of the initial ATP, and an equivalent level of ATP is found that does not bind irreversibly to myosin in a cold chase experiment. A significant level of apparent PIX is observed with subfragment 1 in the fraction that resists washout, and this apparent PIX is shown to be due to contaminant adenylate kinase activity. This apparent PIX due to adenylate kinase provides a possible explanation for the PIX observed by Geeves et al. [Geeves, M. A., Webb, M. R., Midelfort, C. F., & Trentham, D. R. (1980) *Biochemistry 19*, 4748–4754] with subfragment 1.

Positional isotope exchange (PIX)[1] during a reaction provides information on the generation of intermediates that possess rotational freedom [see Rose (1979)]. Thus, cleavage of ATP at the βPO–γP bond leaves the β,γ-bridge oxygen with the ADP, and torsional movement will result in scrambling of this original bridge oxygen with the two original β-nonbridge oxygens. Re-formation of ATP can then occur with incorporation of an original β-nonbridge oxygen into the bridge position. This PIX can be detected by using ATP labeled with

† Supported by Grant AM25980 and an Established Investigatorship from the American Heart Association (to D.D.H.). A preliminary communication has been reported (Dale & Hackney, 1986).
‡ Present address: Department of Biochemistry, University of Texas Health Science Center, San Antonio, TX 78284.

[1] Abbreviations: PIX, positional isotope exchange; PRPP, 5-phospho-D-ribosyl 1-pyrophosphate; Tris, tris(hydroxymethyl)aminomethane; PEP, phosphoenolpyruvate; CaATPase, calcium adenosinetriphosphatase activity of myosin; DAPP, P^1,P^5-di(adenosine-5′) pentaphosphate; S1, myosin subfragment 1; EDTA, ethylenediaminetetraacetic acid; DEAE, diethylaminoethyl; DTT, dithiothreitol; EGTA, ethylene glycol bis(β-aminoethyl ether)-*N,N,N′,N′*-tetraacetic acid.

0006-2960/87/0426-8365$01.50/0